GW and NICER Constraints on Neutron Stars

J. M. Lattimer

Department of Physics & Astronomy

STONY BROOK UNIVERSITY

U.S. DEPARTMENT OF ENERGY
Office of Science

Virtual Meeting on Compact Stars and QCD 2020
ICTS, Tata Institute for Fundamental Research, 17–21 August 2020

Acknowledgements

Funding Support:

US DOE - Nuclear Physics

US DOE - Toward Exascale Astrophysics of Mergers and Supernovae (TEAMS)

NASA - Neutron Star Interior Composition ExploreR (NICER)

NSF - Neutrinos, Nuclear Astrophysics and Symmetries (N3AS)

Recent Collaborators:

Duncan Brown & Soumi De (Syracuse), Christian Drischler (Berkeley), Evgeni Kolomeitsev (Matej Bei, Slovakia), Akira Ohnishi (YITP, Kyoto), Madappa Prakash (Ohio), Achim Schwenk (Darmstadt), Andrew Steiner (Tennessee), Ingo Tews (Los Alamos), Tianqi Zhao & Will Farr (Stony Brook)

Main Topics

- Neutron Stars and How They Depend on the Equation of State
- Maximum Mass and Causality Constraints
- Nuclear Physics and Unitary Gas Constraints
- Measuring Neutron Star Properties From Radio, X-ray and Gravitational Wave Observations
- Estimating Neutron Star Properties from Neutron Star Mergers and NICER

Dany Page
UNAM

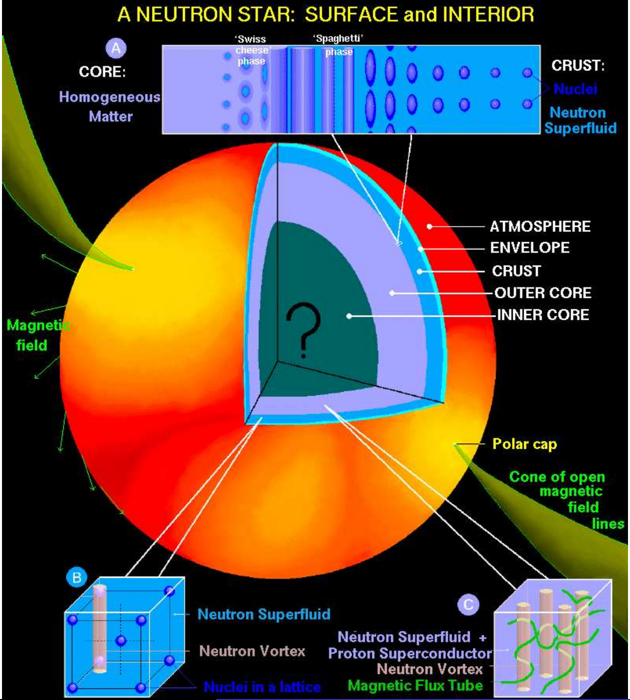

Neutron Star Structure

Tolman-Oppenheimer-Volkov equations

$$\frac{dp}{dr} = -\frac{G}{c^4}\frac{(mc^2 + 4\pi pr^3)(\varepsilon + p)}{r(r - 2Gm/c^2)}$$

$$\frac{dm}{dr} = 4\pi\frac{\varepsilon}{c^2}r^2$$

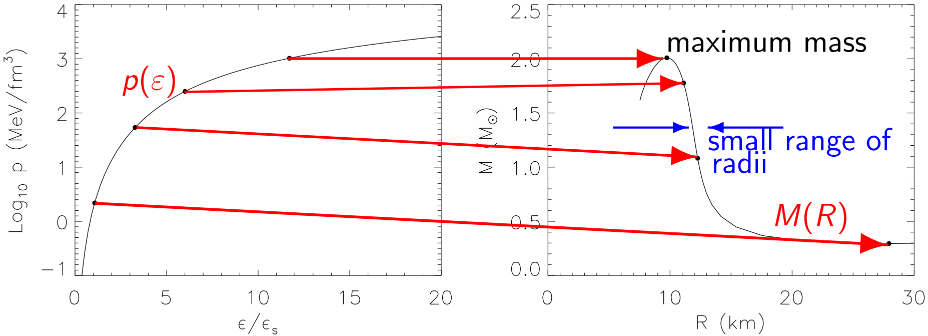

Equation of State ⟵ Observations

Mass-Radius Diagram and Theoretical Constraints

GR:
$R > 2GM/c^2$

$P < \infty$:
$R > (9/4)GM/c^2$

causality:
$R \gtrsim 2.9GM/c^2$

— normal NS
— SQS

— $R_\infty = \frac{R}{\sqrt{1-2GM/Rc^2}}$

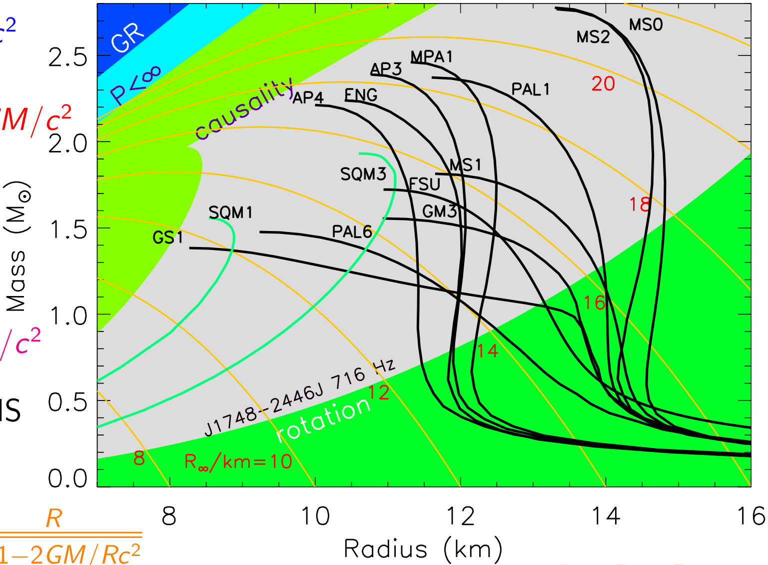

Nuclear Symmetry Energy and the Pressure

The symmetry energy is the difference between the energies of pure neutron matter ($x = 0$) and symmetric ($x = 1/2$) nuclear matter:

$$S(n) = E(n, x = 0) - E(n, x = 1/2)$$

Usually approximated as an expansion around the saturation density (n_s) and isopin symmetry ($x = 1/2$):

$$E(n, x) = E(n, 1/2) + (1-2x)^2 S_2(n) + \dots$$

$$S_2(n) = \mathbf{S_v} + \frac{\mathbf{L}}{3}\frac{n - n_s}{n_s} + \dots$$

$$\mathbf{S_v} \simeq 31 \text{ MeV}, \quad \mathbf{L} \simeq 50 \text{ MeV}$$

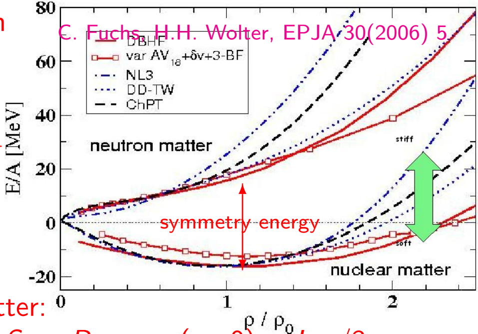

Extrapolated to pure neutron matter:

$$E(n_s, 0) \approx S_v + E(n_s, 1/2) \equiv S_v - B, \qquad p(n_s, 0) = L n_s/3$$

Neutron star matter (beta equilibrium) is nearly neutron matter:

$$\frac{\partial(E + E_e)}{\partial x} = 0, \quad p(n_s, x_\beta) \simeq \frac{L n_s}{3}\left[1 - \left(\frac{4 S_v}{\hbar c}\right)^3 \frac{4 - 3 S_v/L}{3\pi^2 n_s}\right]$$

Bounds From Unitary Gas Conjecture

The Conjecture:
Neutron matter energy is larger than that of the unitary gas $E_{UG} = \xi_0(3/5)E_F$, or

$$E_{UG} \simeq 12.6 \left(\frac{n}{n_s}\right)^{2/3} \mathrm{MeV}$$

The unitary gas consists of fermions interacting via a pairwise short-range s-wave interaction with infinite scattering length and zero range. Cold atom experiments show a universal behavior with the Bertsch parameter $\xi_0 \simeq 0.37$.

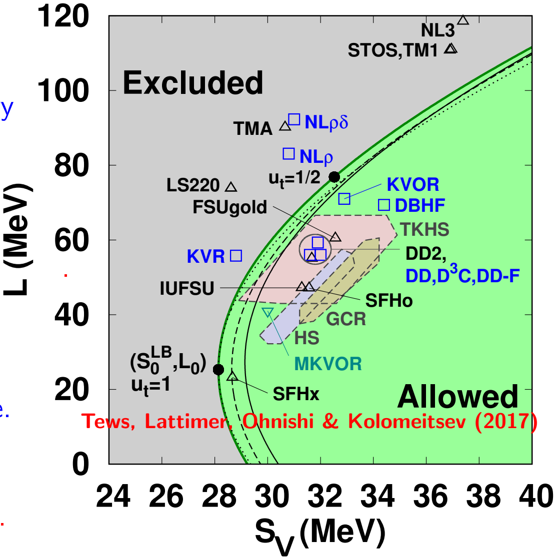

$S_v \geq 28.6$ MeV; $L \geq 25.3$ MeV; $p_0(n_s) \geq 1.35$ MeV fm^{-3}; $R_{1.4} \geq 9.7$ km

Nuclear Experimental Constraints

Masses of Nuclei
surface-volume symmetry energy correlation

Neutron Skin Thickness
$r_{np,208} = 0.15 \pm 0.04$ fm

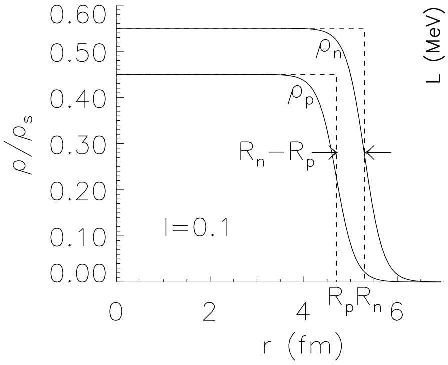

Tarbert et al. (2014)

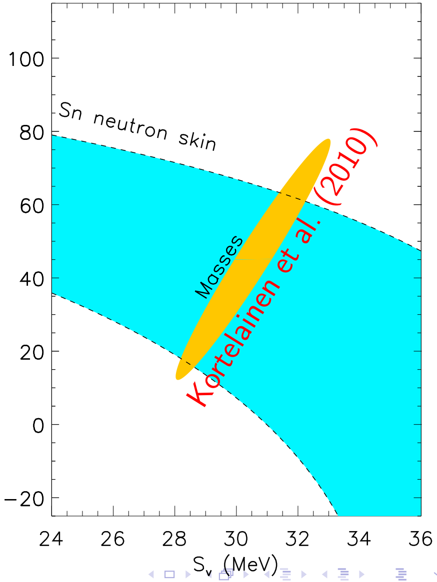

Theoretical and Experimental Constraints

H Chiral Lagrangian

G: Quantum Monte Carlo

neutron matter calculations from Hebeler et al. (2012)

unitary gas constraints from Tews et al. (2017)

Combined experimental constraints are compatible with unitary gas bounds.

Neutron matter calculations are compatible with both.

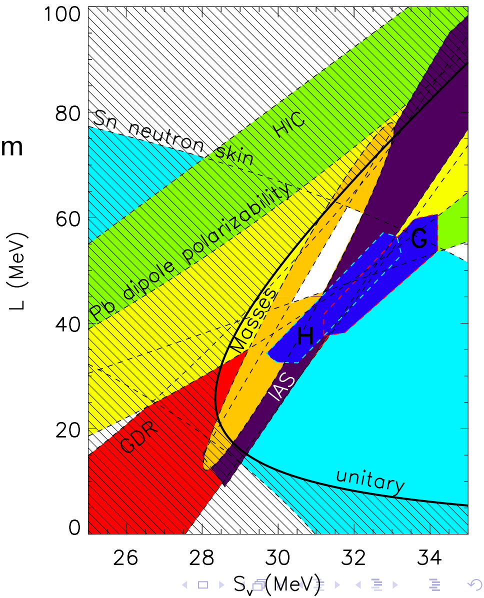

The Radius – Pressure Correlation

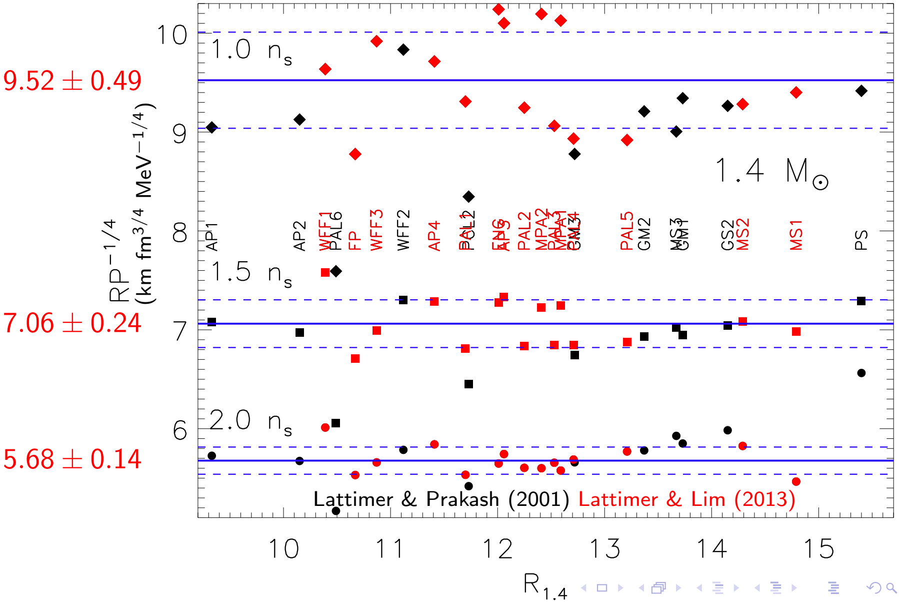

Theoretical and Experimental Constraint Summary

$$R_{1.4} = (9.52 \pm 0.49) \left(\frac{p_s}{\mathrm{MeV\ fm^{-3}}} \right)^{1/4} \mathrm{km}$$

$$p_s \simeq n_s L/3$$

$$30\ \mathrm{MeV} \lesssim L \lesssim 70\ \mathrm{MeV} :$$

$$10.9\ \mathrm{km} \lesssim R_{1.4} \lesssim 13.1\ \mathrm{km}$$

Causality and $M_{max} \gtrsim 2.0 M_\odot$: $R_{1.4} \gtrsim 8.2\ \mathrm{km}$
Imposing the unitary gas conjecture: $R_{1.4} \gtrsim 9.7\ \mathrm{km}$

Measuring Neutron Star Masses and Radii

- Pulsar timing can accurately ($\gtrsim 0.0001 M_\odot$) measure masses.

  Most are between $1.2 M_\odot$ and $1.5 M_\odot$; lowest is $1.174 \pm 0.004 M_\odot$, highest are $2.14^{+0.10}_{-0.09} M_\odot$ and $2.01 \pm 0.04 M_\odot$. Higher estimates have large uncertainties.

- Thermal and bursting observations of X-rays yield radii, but uncertain to a few km.
  - Quiescent sources in globular clusters
  - Thermonuclear explosions on accreting neutron stars in binaries
  - Pulse profile modeling of hot spots on rapidly rotating neutron stars (NICER experiment)

- Gravitational waves from merging neutron stars measure masses and tidal deformabilites.

  GW170817 suggests $R = 11 \pm 1$ km

GW170817

- LIGO-Virgo (LVC) detected a signal consistent with a BNS merger, followed 1.7 s later by a weak sGRB.
- 16600 orbits observed over 165 s.
- $\mathcal{M} = 1.187 \pm 0.001\ M_\odot$
- $M_{\rm T,min} = 2^{6/5}\mathcal{M} = 2.726 M_\odot$
- $E_{\rm GW} > 0.025 M_\odot c^2$
- $D_L = 40 \pm 10$ Mpc
- $75 < \tilde{\Lambda} < 560$ (90%)
- $M_{\rm ejecta} \sim 0.06 \pm 0.02\ M_\odot$
- Blue ejecta: $\sim 0.01 M_\odot$
- Red ejecta: $\sim 0.05 M_\odot$
- Possible r-process production
- Ejecta + GRB: $M_{max} \lesssim 2.2 M_\odot$

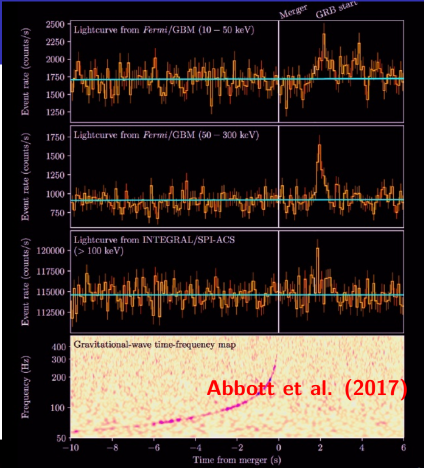

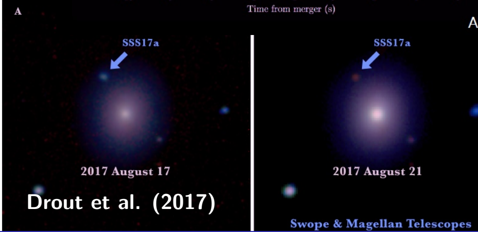

Properties of Known Double Neutron Star Binaries

- Both component masses are accurately measured (11)

— Only the total binary mass is accurately measured (7)

Binaries with $\tau_{GW} > t_{\rm universe}$ (6)

$q = M_2/M_1$ is the binary mass ratio for a system

$\chi = cJ/(GM^2)$ is the dimensionless spin parameter for individual pulsars

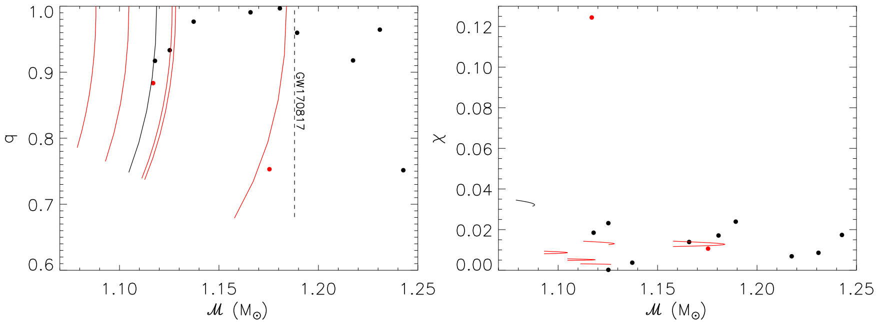

$\mathcal{M} = (M_1 M_2)^{3/5}(M_1 + M_2)^{-1/5}$ is the chirp mass

Binary Merger Gravitational Waveform Models

There are 13 parameters in third PN order $(v/c)^6$ models which include finite-size effects. LVC17 used a 13-parameter model; De et al. (2018) used a 9-10 parameter model.

- Sky location (2) EM data
- Distance (1) EM data
- Inclination (1)
- Coalescence time (1)
- Coalescence phase (1)
- Polarization (1)

} Extrinsic

- Component masses (2)
- Spin parameters (2)
- Tidal deformabilities (2) correlated with masses

} Intrinsic

Tidal Deformability

The tidal deformability λ is the ratio of the induced dipole moment Q_{ij} to the external tidal field E_{ij}, $Q_{ij} \equiv -\lambda E_{ij}$.

We use the dimensionless quantity

$$\Lambda = \frac{\lambda c^{10}}{G^4 M^5} \equiv \frac{2}{3} k_2 \left(\frac{Rc^2}{GM} \right)^5$$

k_2 is the dimensionless Love number.

For a neutron star binary, the mass-weighted $\tilde{\Lambda}$ is the relevant parameter:

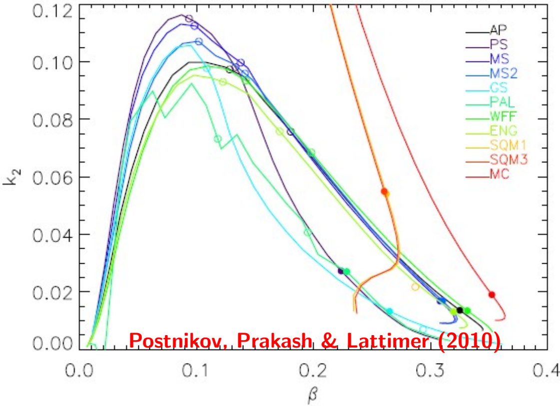

$$\tilde{\Lambda} = \frac{16}{13} \frac{(1+12q)\Lambda_1 + (12+q)q^4\Lambda_2}{(1+q)^5}, \qquad q = M_2/M_1 \le 1$$

The Effect of Tides

Tides accelerate the inspiral and produce a phase shift compared to the case of two point masses.

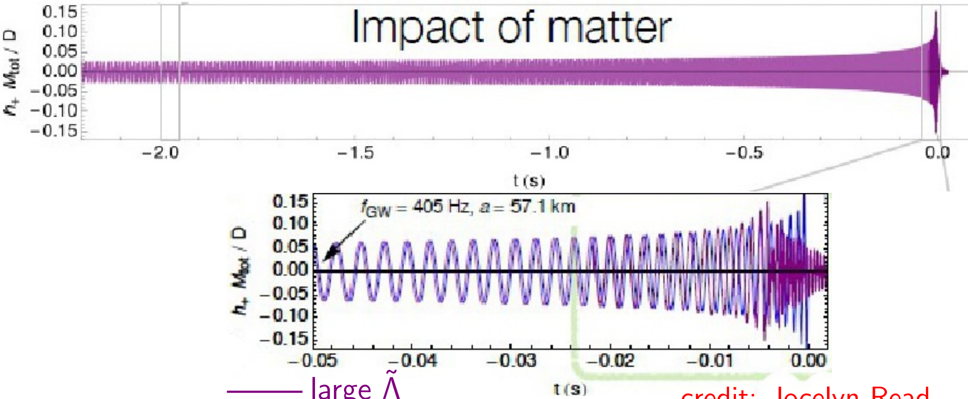

large $\tilde{\Lambda}$

small $\tilde{\Lambda}$

credit: Jocelyn Read

$$\delta\Phi_t = -\frac{117}{256}\frac{(1+q)^4}{q^2}\left(\frac{\pi f_{GW} G\mathcal{M}}{c^3}\right)^{5/3}\tilde{\Lambda} + \cdots .$$

Λ is Highly Correlated With M and R

- $\Lambda = a\beta^{-6}$
  $\beta = GM/Rc^2$

  $a = 0.0086 \pm 0.0011$
  for
  $M = (1.35 \pm 0.25)\ M_\odot$

- If $R_1 \simeq R_2 \simeq R_{1.4}$
  it follows that
  $\Lambda_2 \simeq q^{-6}\Lambda_1$.

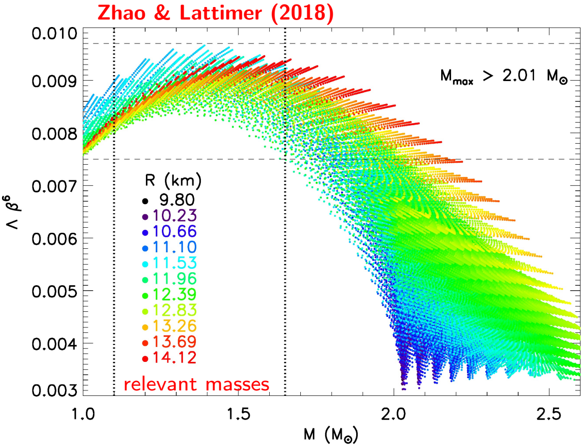

Binary Deformability and the Radius

$$\tilde{\Lambda} = \frac{16}{13}\frac{(1+12q)\Lambda_1 + q^4(12+q)\Lambda_2}{(1+q)^5} \simeq \frac{16a}{13}\left(\frac{R_{1.4}c^2}{G\mathcal{M}}\right)^6 \frac{q^{8/5}(12-11q+12q^2)}{(1+q)^{26/5}}$$

- $\tilde{\Lambda} = a'(R_{1.4}c^2/G\mathcal{M})^6$
  $a' = 0.0035 \pm 0.0006$
  for
  $\mathcal{M} = (1.2 \pm 0.2)\ M_\odot$
- For GW170817:
  $a' = 0.00375 \pm 0.00025$
- $R_{1.4} =$
  $(11.5 \pm 0.3)\dfrac{\mathcal{M}}{M_\odot}\left(\dfrac{\tilde{\Lambda}}{800}\right)^{1/6}$ km
- For GW170817:
  $R_{1.4} = (13.4 \pm 0.1)\left(\dfrac{\tilde{\Lambda}}{800}\right)^{1/6}$ km

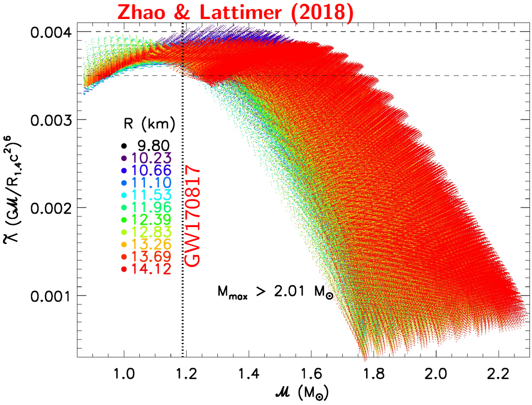

68.3%, 90%, 95.4% and 99.7% Confidence Bounds

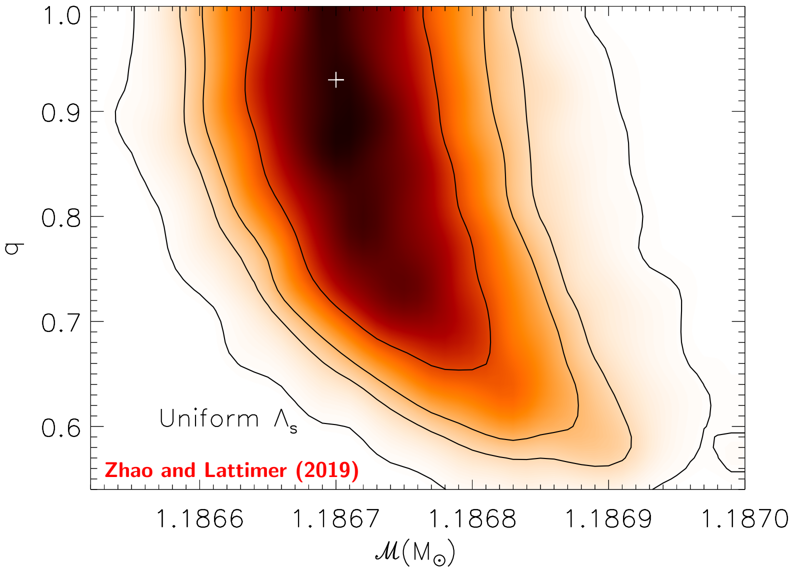

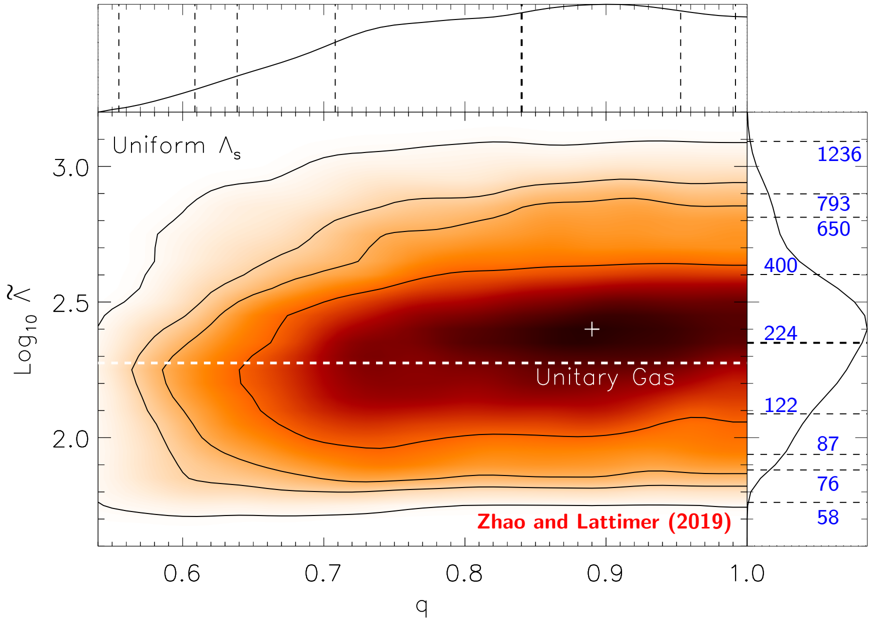
Uniform Λ_s
3.0
2.5
2.0
$\text{Log}_{10}\,\tilde{\Lambda}$
0.6
0.7
0.8
0.9
1.0
q
Unitary Gas
Zhao and Lattimer (2019)
1236
793
650
400
224
122
87
76
58

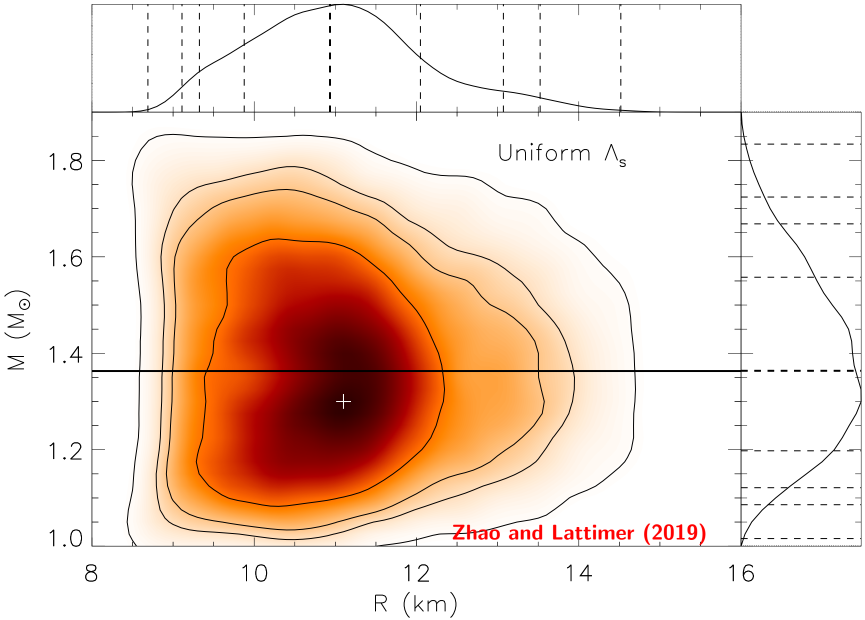
Uniform Λ_s
Zhao and Lattimer (2019)
1.8
1.6
1.4
1.2
1.0
M ($M_\odot$)
8
10
12
14
16
R (km)

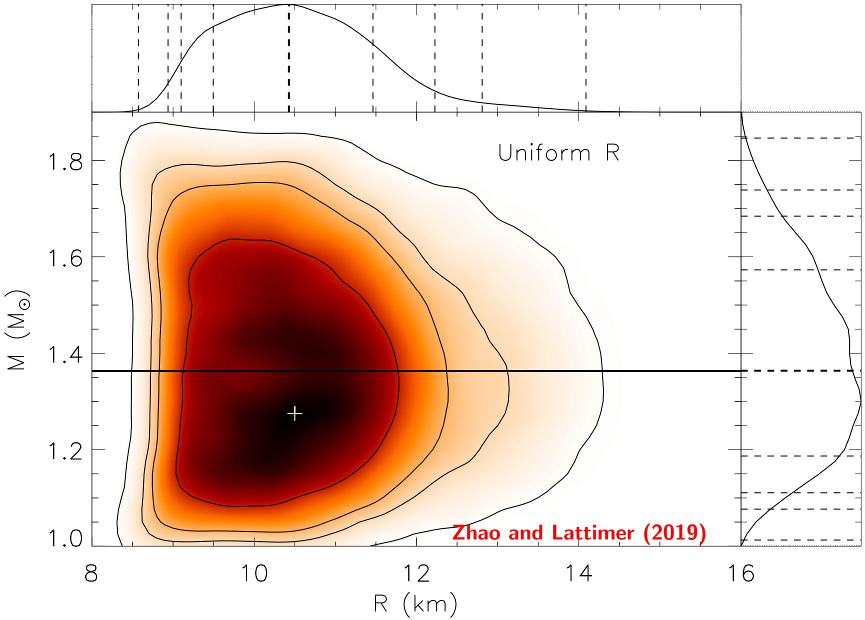

Uniform R
Zhao and Lattimer (2019)
1.8
1.6
1.4
1.2
1.0
M (M⊙)
8
10
12
14
16
R (km)

Maximum Mass Constraint From GW170817

- Pulsar observations imply non-rotating $M_{max} \gtrsim 2M_\odot$.
- Remnant differential rotation uniformizes within ~ 0.1s.
- Inspiralling mass $M_T = \mathcal{M}q^{-3/5}(1+q)^{6/5}$ is $2.73M_\odot$ $(q=1)$ to $2.78M_\odot$ $(q=0.7)$, smaller than $M_{max,d}$.
- Maximally uniformly rotating stars have $M_{max,u} = \xi M_{max}$ with $1.17 \lesssim \xi \lesssim 1.21$. *Hypermassive* stars, with $M_T > M_{max,u}$, promptly collapse to a BH.
- *Supermassive* stars, with $M_{max} \leq M_T \leq M_{max,u}$, are metastable but have much longer lifetimes. Such a remnant pumps too much energy into the ejecta to be consistent with observations.
- Taking into account gravitational binding energy, the condition $M_T > M_{max,u}$ implies $M_{max} \leq 2.25M_\odot$.

Neutron Star Interior Composition ExploreR (NICER)

Science Measurements NICER

Reveal stellar structure through lightcurve modeling, long-term timing, and pulsation searches

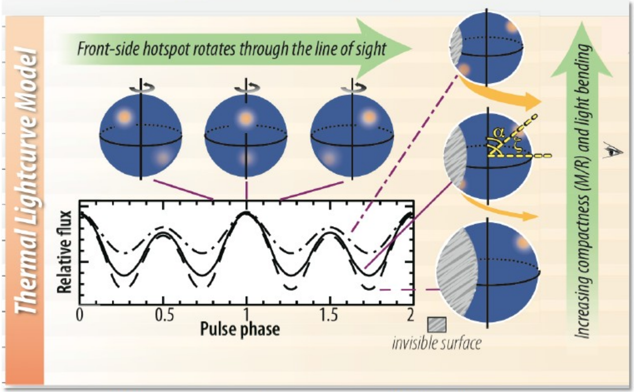

Lightcurve modeling constrains the compactness (M/R) and viewing geometry of a non-accreting millisecond pulsar through the depth of modulation and harmonic content of emission from rotating hot-spots, thanks to gravitational light-bending…

Science Measurements (cont.)

NICER

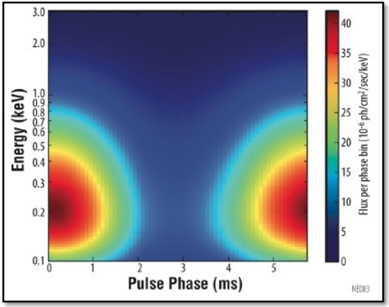

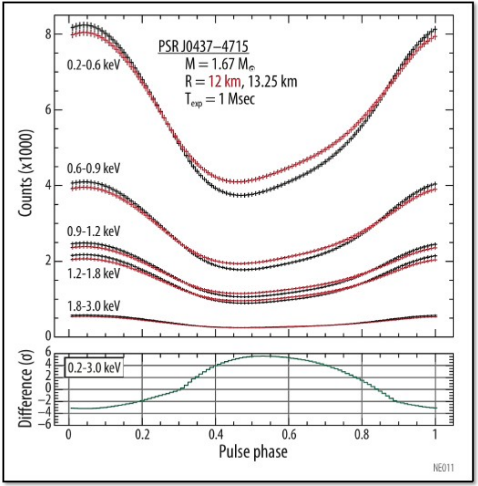

… while phase-resolved spectroscopy promises a direct constraint of radius *R*.

NICER Results For PSR J0030+0451

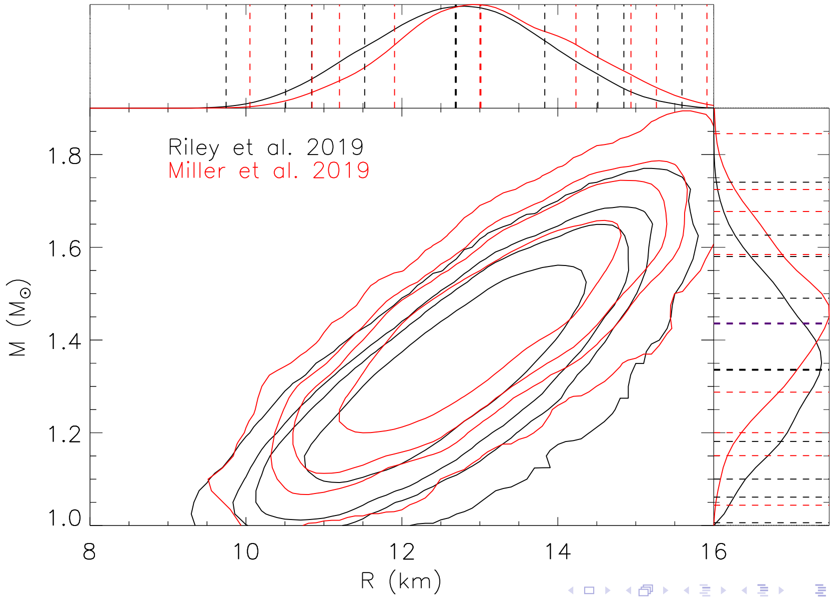

Comparison of GW and NICER Results

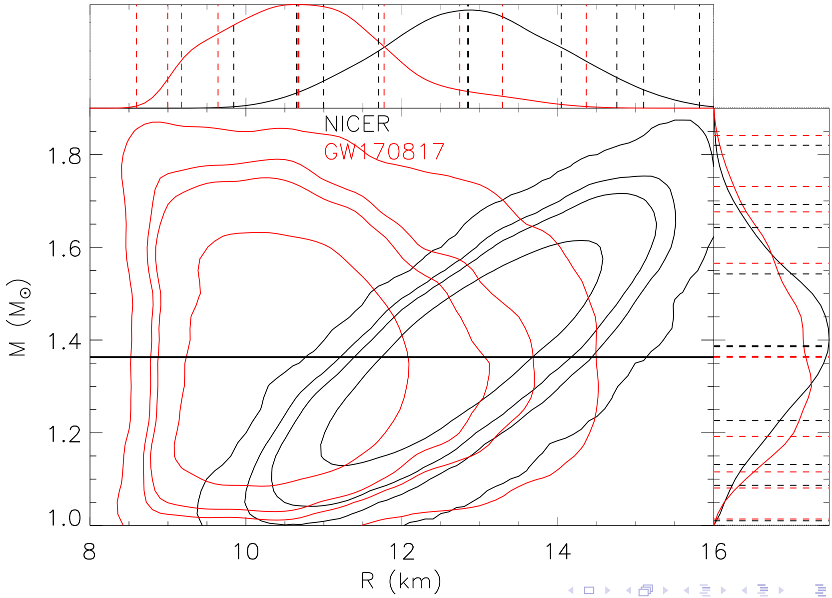

Composite of GW and NICER Results

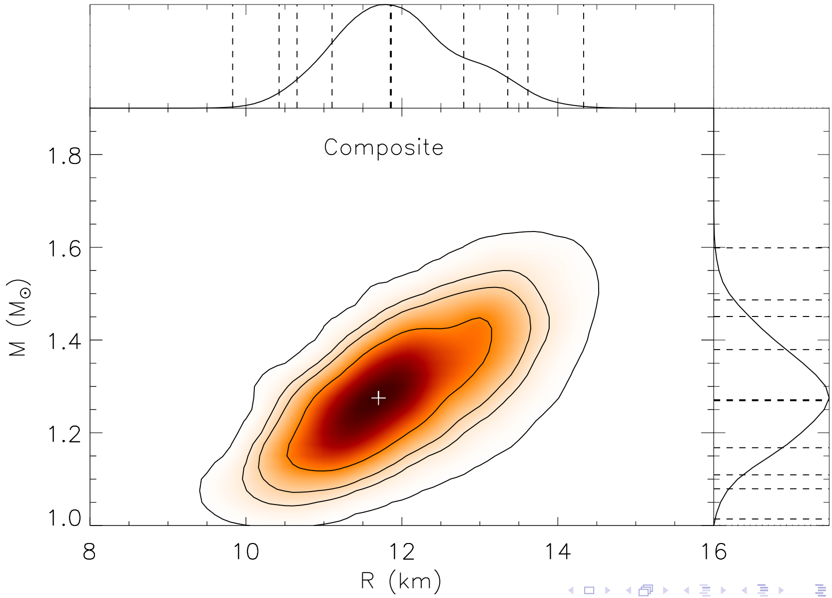

LVC O3 Detections

28 BBH systems (1 is marginal); 1 may contains a $2.6M_\odot$ BH

- GW190814 (267 ± 52 Mpc, FAR$=2.0 \cdot 10^{-33}$, $\mathcal{M} = 6.09 \pm 0.06 M_\odot$, $q = 0.112 \pm 0.009$)

1 probable BHNS with a $2.3M_\odot$ BH and a $1.2M_\odot$ NS (alternative is a BNS with $2 \sim 1.7M_\odot$ NSs)

- GW190425 (156 ± 41 Mpc, FAR $= 4.5 \cdot 10^{-13}$, $\mathcal{M} = 1.44 \pm 0.02 M_\odot$, $\tilde{\Lambda} \leq 900$, $R < 16$ km)

3 other BHNS systems, all of which are marginal

- GW190426 (377 ± 100 Mpc, FAR $= 1.9 \cdot 10^{-8}$, $M_{\rm BH} \sim 6M_\odot$, $M_{\rm NS} \sim 1.3M_\odot$)
- GW190910 (632 ± 186 Mpc, FAR $= 3.7 \cdot 10^{-9}$)
- GW191205 (385 ± 164 Mpc, FAR $1.2 \cdot 10^{-8}$)

4 BNS systems, all of which are marginal

- GW191213 (201 ± 81 Mpc, FAR $= 3.5 \cdot 10^{-8}$)
- GW190510 (1331 ± 341 Mpc, FAR $= 8.8 \cdot 10^{-10}$)
- GW190901 (241 ± 79 Mpc, FAR $= 7.0 \cdot 10^{-9}$)
- GW190910 (241 ± 89 Mpc, FAR $= 3.6 \cdot 10^{-8}$)

Summary

- GW170817 provided R and EOS information compatible with expectations from nuclear theory, experiment and other astrophysical observations, considering existing systematic uncertainties.
- GW170817 also hints that M_{max} is not far above the $2M_\odot$ minimum provided by pulsar timing, supported by possible identification of low-mass black holes with $M < 3M_\odot$.
- NICER provides consistent radius information from pulse-profile models of rapidly rotating X-ray pulsars.
- Future GW measurements of BNS will be additive since sources should be similar.